Materials Science and Engineering C 63 (2016) 231–239

Contents lists available at ScienceDirect

Materials Science and Engineering C

journal homepage: www.elsevier.com/locate/msec

Encapsulation of gallic acid/cyclodextrin inclusion complex in electrospun polylactic acid nanofibers: Release behavior and antioxidant activity of gallic acid

Zeynep Aytac [a,b], Semran Ipek Kusku [b,c], Engin Durgun [a,b], Tamer Uyar [a,b,*]

[a] Institute of Materials Science & Nanotechnology, Bilkent University, Ankara 06800, Turkey
[b] UNAM-National Nanotechnology Research Center, Bilkent University, Ankara 06800, Turkey
[c] Department of Engineering Physics, Istanbul Medeniyet University, Göztepe 34700, Istanbul, Turkey

ARTICLE INFO

Article history:
Received 25 December 2015
Received in revised form 3 February 2016
Accepted 22 February 2016
Available online 26 February 2016

Keywords:
Electrospinning
Polylactic acid
Gallic acid
Hydroxypropyl-beta-cyclodextrin
Release
Antioxidant activity

ABSTRACT

Cyclodextrin-inclusion complexes (CD-ICs) possess great prominence in food and pharmaceutical industries due to their enhanced ability for stabilization of active compounds during processing, storage and usage. Here, CD-IC of gallic acid (GA) with hydroxypropyl-beta-cyclodextrin (GA/HPβCD-IC) was prepared and then incorporated into polylactic acid (PLA) nanofibers (PLA/GA/HPβCD-IC-NF) using electrospinning technique to observe the effect of CD-ICs in the release behavior of GA into three different mediums (water, 10% ethanol and 95% ethanol). The GA incorporated PLA nanofibers (PLA/GA-NFs) were served as control. Phase solubility studies showed an enhanced solubility of GA with increasing amount of HPβCD. The detailed characterization techniques (XRD, TGA and ^{1}H-NMR) confirmed the formation of inclusion complex between GA and HPβCD. Computational modeling studies indicated that the GA made an efficient complex with HPβCD at 1:1 either in vacuum or aqueous system. SEM images revealed the bead-free and uniform morphology of PLA/GA/HPβCD-IC-NF. The release studies of GA from PLA/GA/HPβCD-IC-NF and PLA/GA-NF were carried out in water, 10% ethanol and 95% ethanol, and the findings revealed that PLA/GA/HPβCD-IC-NF has released much more amount of GA in water and 10% ethanol system when compared to PLA/GA-NF. In addition, GA was released slowly from PLA/GA/HPβCD-IC-NF into 95% ethanol when compared to PLA/GA-NF. It was also observed that electrospinning process had no negative effect on the antioxidant activity of GA when GA was incorporated in PLA nanofibers.

© 2016 Elsevier B.V. All rights reserved.

1. Introduction

Phenolic compounds are the most common primary antioxidants to readily scavenge free radicals by donating hydrogen atom or an electron [1]. GA is a hydroxybenzoic acid and considered as a natural phenolic antioxidant and antimicrobial agent (Fig. 1a). GA and its derivatives including tannins and catechin are especially found in berries, citrus fruits, cereals, tea, wine and herbs [2]. Since it has antioxidant and antimicrobial activity, it is used as an additive in food, cosmetics and pharmaceutical industry [3–6]. However, it might easily oxidize which further leads to degradation. Cyclodextrin (CD) (Fig. 1b), as an enzyme-modified starch derivative, is nontoxic, biodegradable, and environmentally benign. CDs have truncated-cone shape structure with a lipophilic cavity (Fig. 1c). Due to the presence of cavity and high recognition ability of CDs toward various guest molecules, stable CD-inclusion complexes (ICs) can be obtained by nonpolar molecules. The driving forces of host-guest binding are mainly due to the release of enthalpy-rich water molecules from cavity and non-covalent interactions including van der Waals interactions, hydrogen bonding, and hydrophobic interactions [7]. Therefore CD-ICs are helpful in numerous areas for improving the stability against oxygen, temperature and light; the solubility, controlling the release of guest compounds, masking malodors [7]. In order to protect GA for degradation and maintain its bioactivity against external and environmental factors, CD-IC has been synthesized and considered to be an efficient system in recent years [8–9]. Therefore stabilization of GA might be improved by an encapsulation technique, inclusion complexation. CD-IC has gained great potential to enhance the shelf life of foods, increase the solubility of hydrophobic food additives and drugs and suppress unpleasant odors and tastes in food products and drug formulations even though there are many different commercial methods that are currently followed for the stabilization of chemicals.

Among nanofiber production methods, electrospinning has been recognized as simple and cost-effective method [10–12]. Various polymeric nanofibers have been already produced by using electrospinning technique. In addition to that, flexibility of this process enables to obtain nanofibers containing active agents which have potential to be used in diverse application areas [13–14]. Therefore, gallic acid encapsulated

* Corresponding author at: Institute of Materials Science & Nanotechnology, Bilkent University, Ankara 06800, Turkey.
E-mail address: tamer@unam.bilkent.edu.tr (T. Uyar).

http://dx.doi.org/10.1016/j.msec.2016.02.063
0928-4931/© 2016 Elsevier B.V. All rights reserved.

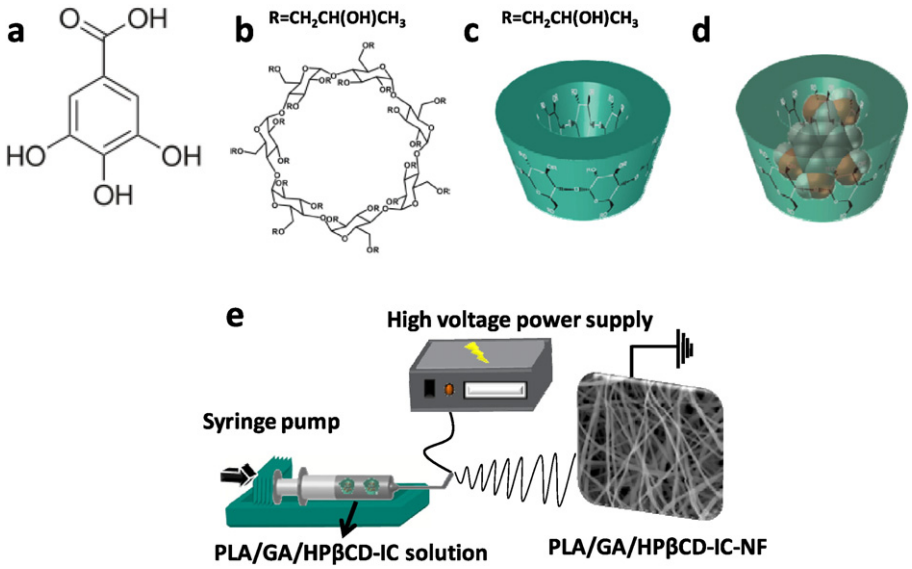

Fig. 1. Chemical structure of (a) GA, (b) HPβCD; schematic representation of (c) HPβCD, (d) the GA/HPβCD-IC formation and (e) electrospinning of nanofibers from PLA/GA/HPβCD-IC solution.

polymeric films and electrospun nanofibers have been studied previously [3,5,15–16]. CD-ICs can be incorporated into polymeric films and then CD-IC functionalized polymeric films might be used in food packaging and pharmaceutical applications [17]. However, designing delivery systems for food packaging and drug delivery applications by using nanofibers is advantageous over films owing to the high surface area and highly porous structure. In one of our study, sulfisoxazole (SFS)/CD-IC incorporated hydroxypropyl cellulose (HPC) nanofibers (HPC/SFS/CD-IC-NF) and films (HPC/SFS/CD-IC-film) were produced. The release of SFS was much more but slower from HPC/SFS/CD-IC-NF as compared to HPC/SFS/CD-IC-film. Low surface area of HPC/SFS/CD-IC-film and close location of SFS to the surface in HPC/SFS/CD-IC-film was stated the reason of less amount and quick release of SFS from HPC/SFS/CD-IC-film [18]. Polylactic acid (PLA) is a biodegradable aliphatic polyester produced from L-lactic acid and well suited for food packaging and drug delivery applications owing to its biocompatibility, biodegradability; carbon dioxide, oxygen and water permeability, and light barrier properties [19]. Leading studies related to incorporation of CD-IC of various guest molecules into electrospun nanofibers were reported by our research group [18,20–28].

In this paper, IC of GA and HPβCD (GA/HPβCD-IC) (Fig. 1d) was formed and then it was incorporated into PLA nanofibers (PLA/GA/HPβCD-IC-NF) by electrospinning technique (Fig. 1e). The prepared GA/HPβCD-IC was characterized by using phase solubility, X-ray diffraction (XRD), thermogravimetric analysis (TGA), and proton nuclear magnetic resonance (^{1}H NMR). Computational modeling studies were also performed to investigate complexation in vacuum and in aqueous system. GA incorporated PLA nanofibers without HPβCD (PLA/GA-NF) were taken as a control sample. The morphological characterization of PLA/GA-NF and PLA/GA/HPβCD-IC-NF were carried out by scanning electron microscope (SEM). The release of GA from PLA/GA/HPβCD-IC-NF and PLA/GA-NF was determined in aqueous solution, 10% ethanol, and 95% ethanol by high performance liquid chromatography (HPLC). The antioxidant activity of the GA presented in PLA/GA/HPβCD-IC-NF and PLA/GA-NF was evaluated using 2,2-diphenyl-1-picrylhydrazyl (DPPH) radical scavenging method.

2. Experimental

2.1. Materials

Polylactic acid (PLA) was donated by Natureworks (product code 6252D). Gallic acid (GA, ≥97.5–102.5%, Sigma Aldrich), hydroxypropyl-beta-cyclodextrin (HPβCD, Wacker Chemie AG, Germany), methanol (extra pure, Sigma Aldrich), ethanol (99.8%, Sigma Aldrich), dichloromethane (DCM, extra pure, Sigma Aldrich), N,N-dimethylformamide (DMF, ≥99%, Sigma Aldrich), acetonitrile (ACN, chromasol, Sigma Aldrich), deuterated dimethylsulfoxide (DMSO-d6, deuteration degree min 99.8% for NMR spectroscopy, Merck), and 2,2-diphenyl-1-picrylhydrazyl (DPPH, Sigma Aldrich) were purchased and used as-received without any further purification. Distilled–deionized water was supplied from Millipore milli-Q ultrapure water system.

2.2. Preparation of inclusion complex (IC) and physical mixture (PM) of GA and HPβCD (GA/HPβCD-IC and GA/HPβCD-PM)

The formation of solid GA/HPβCD-IC was prepared according to slurry method. Initially, GA was dissolved in aqueous solution; then HPβCD was added and the mixture was stirred for 120 min at 70 °C. The mixture was kept in hood for 2 days and the resulting white powder was crashed in agate mortar. The molar ratio of GA:HPβCD was used as 1:1. GA/HPβCD-PM was obtained by mixing GA and HPβCD in a glass mortar at a molar ratio of 1:1.

2.3. Preparation of electrospinning solutions

Free GA and GA/HPβCD-IC incorporated PLA nanofibers (PLA/GA-NF and PLA/GA/HPβCD-IC-NF) were produced via electrospinning technique. For this purpose, Free GA (5%, w/w, with respect to polymer) was dissolved in DCM:DMF (7:3) at room temperature (RT). Then, 10% PLA (w/v) was added and PLA/GA solution was stirred for 120 min before electrospinning. With regard to PLA/GA/HPβCD-IC-NF, GA/HPβCD-IC (5% GA, w/w, with respect to polymer) was dispersed in DCM:DMF (7:3) at RT. Afterwards, 10% PLA (w/v) was added, PLA/GA/HPβCD-IC solution was stirred 120 min prior to electrospinning. The vials were covered with a piece of aluminum foil during stirring to avoid any potential light effect for GA. As a reference sample, we have also electrospun 10% PLA solution (w/v) prepared in DCM:DMF (7:3). Table 1 summarizes the composition of the PLA, PLA/GA and PLA/GA/HPβCD-IC solutions and the morphological findings of PLA-NF, PLA/GA-NF and PLA/GA/HPβCD-IC-NF.

2.4. Electrospinning

PLA, PLA/GA and PLA/GA/HPβCD-IC solutions loaded into 3 ml plastic syringe with a needle inner diameter of 0.8 mm were placed horizontally

Table 1
The properties of the solutions used for electrospinning and morphological characteristics of the resulting nanofibers.

Solutions	% PLA[a] (w/v)	% HPβCD[b] (w/w)	% GA[b] (w/w)	Viscosity (Pa·s)	Conductivity (μS/cm)	Average fiber diameter (nm)	Fiber morphology
PLA	10	–	–	0.15	0.16	320 ± 115	Bead free nanofibers
PLA/GA	10	–	5	0.18	0.30	495 ± 105	Bead free nanofibers
PLA/GA/HPβCD-IC	10	43	5	0.22	14.13	235 ± 65	Bead free nanofibers

[a] with respect to solvent (DCM:DMF, 7:3).
[b] with respect to polymer (PLA).

on the pump. The solutions were sent towards to the collector at 1 ml/h rate by syringe pump (KD Scientific, KDS101). 15 kV was applied from a high voltage power supply (AU Series, Matsusada Precision Inc.). Cylindrical metal covered with aluminum foil was used as a collector. Distance between needle tip and collector was 10 cm. Experiments were performed at 24–25 °C, 17–18% humidity.

2.5. Characterizations and measurements

Phase solubility measurements were performed in aqueous solution according to the method of Higuchi and Connors [29]. Excess amount of GA was added to 10 ml of water containing HPβCD (ranging from 0 to 0.016 M). The equilibrium was achieved by stirring the solutions for 12 h at RT, the suspensions were filtered through 0.45 μm membrane filter to remove undissolved solid. GA concentration was determined spectrophotometrically at 259 nm (Varian, Cary 100). The stability constant (K_S) of the complex was calculated from the phase solubility diagram according to the following equation:

$$Ks = \text{slope}/S_0(1-\text{slope}) \quad (1)$$

where S_0 is the solubility of GA in the absence of HPβCD. The phase solubility diagram is a plot of the molar concentration of GA versus molar concentration of HPβCD.

The crystalline structure of powder of GA, HPβCD, GA/HPβCD-IC and GA/HPβCD-PM were recorded via X-ray diffraction (XRD, PANalytical X'Pert powder diffractometer) applying Cu Kα radiation in a 2θ range 5°–30°.

Thermal gravimetric analysis (TGA, TA Q500, USA) was used to investigate the thermal properties of GA, HPβCD, GA/HPβCD-IC and GA/HPβCD-PM in high resolution TGA mode (dynamic rate). The measurements were carried out under nitrogen atmosphere, and the samples were heated up to 500 °C at a constant heating rate of 20 °C/min.

The proton nuclear magnetic resonance (^{1}H-NMR) spectra were recorded on Bruker DPX-400 at 400 MHz. 10 mg of GA, HPβCD and GA/HPβCD-IC was dissolved in 0.5 ml of d6-DMSO to evaluate the molar ratio of GA/HPβCD-IC. Integration of the chemical shifts (δ) given in parts per million (ppm) was calculated by using Mestrenova software.

In order to investigate how the solution parameters affect the diameter of the nanofibers, viscosity and conductivity measurements were done at RT. The viscosity of PLA, PLA/GA and PLA/GA/HPβCD-IC solutions were analyzed via Anton Paar Physica MCR 301 rheometer equipped with a cone/plate accessory (spindle type CP40-2) at a constant shear rate of 100 1/sec and the conductivity of the above-mentioned solutions was measured with Inolab 720-WTW.

The morphology of PLA-NF, PLA/GA-NF and PLA/GA/HPβCD-IC-NF was investigated by scanning electron microscopy (SEM, FEI-Quanta 200 FEG). Samples were mounted on metal stubs with double-sided adhesive copper tape and coated with 5 nm Au/Pd (PECS-682). Average fiber diameter (AFD) of the nanofibers was calculated from the SEM micrographs. At least 100 fibers were measured for each sample, and their averages and standard deviations were reported.

The cumulative amount of released GA from PLA/GA-NF and PLA/GA/HPβCD-IC-NF was measured via high performance liquid chromatography (HPLC, Agilient, 1200 series) equipped with VWD UV detector and the detection was accomplished at 259 nm. Nanofibers (20 mg) were individually immersed in 30 ml of aqueous solution, 10% ethanol and 95% ethanol and the solutions were stirred at RT at 50 rpm for 240 min. The three mediums were used to observe the release of GA in mediums having different polarities. In addition, these three different mediums (water, 10% ethanol and 95% ethanol) are aqueous, alcoholic and fatty food simulants, respectively. 0.5 ml of sample solution was withdrawn at specified time intervals and an equal amount of fresh medium was refilled. The diol column (250 mm × 4.6 mm i.d., 5μm, Inertisil GL Sciences Inc.) operating at 1 ml/min with ACN:water (50:50) eluent was used for chromatographic separation. The calibration curves were obtained by dissolving GA in aqueous solution, 10% ethanol and 95% ethanol. The cumulative amount of GA released from nanofibers was converted to concentration (ppm) according to the calibration curves. The experiments were performed in triplicate and the results were reported as average values ± standard deviation. The loading efficiency (LE) (%) of PLA/GA-NF and PLA/GA/HPβCD-IC-NF were determined by dissolving certain amount of nanofiber in DCM:DMF (7:3) and the amount of GA in the nanofiber was determined by HPLC using the calibration curve obtained in DCM:DMF (7:3) in triplicate. Finally, loading efficiency (%) was calculated according to the following equation:

$$\text{Loading efficiency (LE) (\%)} = C_e/C_t \times 100 \quad (2)$$

where C_e is the concentration of encapsulated active compound and C_t is the total concentration of active compound.

Antioxidant tests for PLA-NF, PLA/GA-NF and PLA/GA/HPβCD-IC-NF were performed via 2,2-diphenyl-1-picrylhydrazyl (DPPH) radical scavenging assay. The nanofibers having equivalent amount of GA were immersed in 3 ml of 10^{-4} M DPPH solution prepared in methanol in dark for 30 min at RT. The mixtures were incubated in the dark at RT for 15 min. The absorbance of the solutions was measured by UV–Vis NIR spectroscopy (Varian, Cary 5000) at 517 nm. The absorbance of DPPH was defined as 100% and the antioxidant activities (%) were calculated according to the following equation:

$$\text{Antioxidant activity (\%)} = \left(A_{\text{control}} - A_{\text{sample}}\right)/A_{\text{control}} * 100 \quad (3)$$

where $A_{control}$ and A_{sample} represent the absorbance values of control DPPH solution and DPPH solution with nanofibers, respectively. The experiments were carried out in triplicate and the results were given as average values ± standard deviation.

2.6. Computational method

We have performed ab initio calculations [30–31] within the generalized gradient approximation [32] including van der Waals correction [33], as implemented in the Vienna ab initio simulation package [34–35]. The pseudopotentials of all elements were described by projector augmented-wave method (PAW) [36] using a plane-wave basis set with a kinetic energy cutoff of 520 eV. The initial structure of HPβCD was obtained from Cambridge Structural Database [37]. The guest molecule (GA), bare HPβCD, and their IC were relaxed in vacuum using the conjugate gradient algorithm without any constraints by setting convergence criteria on the total energy and force to 10^{-4} eV and 10^{-2} eV/Å, respectively. In addition, as the existence of solvent could

alter the inclusion complex formation dynamics by effecting intermolecular interactions, we also considered the solvent (water in this case) effect which is entirely based on implicit solvent model [38]. Combined with ab initio methods, this model splits the system into an explicit part for solute, which is, treated quantum mechanically and an implicit part for solvent treated as a continuum. This solvent model takes into account dispersive interactions [39] and implemented in VASPsol code [40–41].

3. Results and discussion

3.1. Phase solubility studies

Phase solubility diagram obtained for GA/HPβCD complex within the concentration range studied displayed typical A_L type diagram (i.e. linear increment in the solubility of GA as a function of CD concentration), consistent with 1:1 molecular complex formation (Fig. 2a).

The stability constant (K_c) is an important index associated with the drug release and represents the binding strength between guest and host (CD) [42]. K_c determined according to Eq. (1) for GA/HPβCD complex was 100 M^{-1}, suggesting a weak interaction between GA and HPβCD. This weak interaction might be because of the electrostatic interaction between solvent and GA nearby HPβCD cavity as explained in modeling study.

3.2. Crystalline structure of inclusion complex

XRD analysis is used for the detection of inclusion complex formation between guest and host (CD) molecules. In the case of inclusion complexation, the guest molecules are separated from each other due to the presence of CD cavities; so it is not possible to detect the crystalline peaks of guest molecules [43]. XRD patterns of GA, HPβCD, GA/HPβCD-IC and GA/HPβCD-PM are shown in Fig. 2b. Several intense and sharp diffraction peaks at 2θ values of 16.68°, 25.54° and 27.85° were observed in the diffraction pattern of GA. In contrast, no sharp peaks were observed in the diffraction pattern of HPβCD; instead halo-pattern was recorded which is characteristic for amorphous compounds. We observed the characteristic crystalline peaks of GA with less intensity in the diffraction pattern of GA/HPβCD-PM whereas no such peaks were observed in the case of GA/HPβCD-IC. Therefore, the disappearance of characteristic peaks of GA confirms the interaction between GA and HPβCD and further leads to a conclusion that GA was probably included in the cavity of HPβCD [44].

3.3. Thermal analysis of inclusion complex

GA/HPβCD-IC was further investigated by Hi-Res TGA to determine the thermal stability (Fig. 2c). Hi-Res TGA of GA, HPβCD and GA/HPβCD-PM was also shown for reference. GA exhibited two steps of weight loss, between 210 °C and 325 °C which correspond to the decomposition of GA. HPβCD lost weight in two distinct steps, the former was loss of water molecules that are in the cavity; the latter that is after 295 °C was the main decomposition of HPβCD. In the case of GA/HPβCD-PM, there exist three weight losses which can be attributed to water, GA; GA and HPβCD, respectively. The first weight loss occurred at temperatures below 100 °C; the second and third weight losses range between 200 °C to 250 °C and 270 °C to 400 °C. So, the onset of thermal degradation of GA has decreased slightly. GA/HPβCD-IC exhibited weight losses in three stages. The first weight loss that occurred at temperatures below 100 °C can be ascribed to the water loss; the second and third weight losses that range from 210 °C to 250 °C and 265 °C to 400 °C might correspond to GA and HPβCD, respectively. So, it is concluded that the thermal stability of GA did not alter by complexation in contrast to GA/HPβCD-PM. The observed results further confirm the complex formation [45]. In addition, the amount of GA in GA/HPβCD-IC and GA/HPβCD-PM were determined as ~10.2 % and ~9.4% from

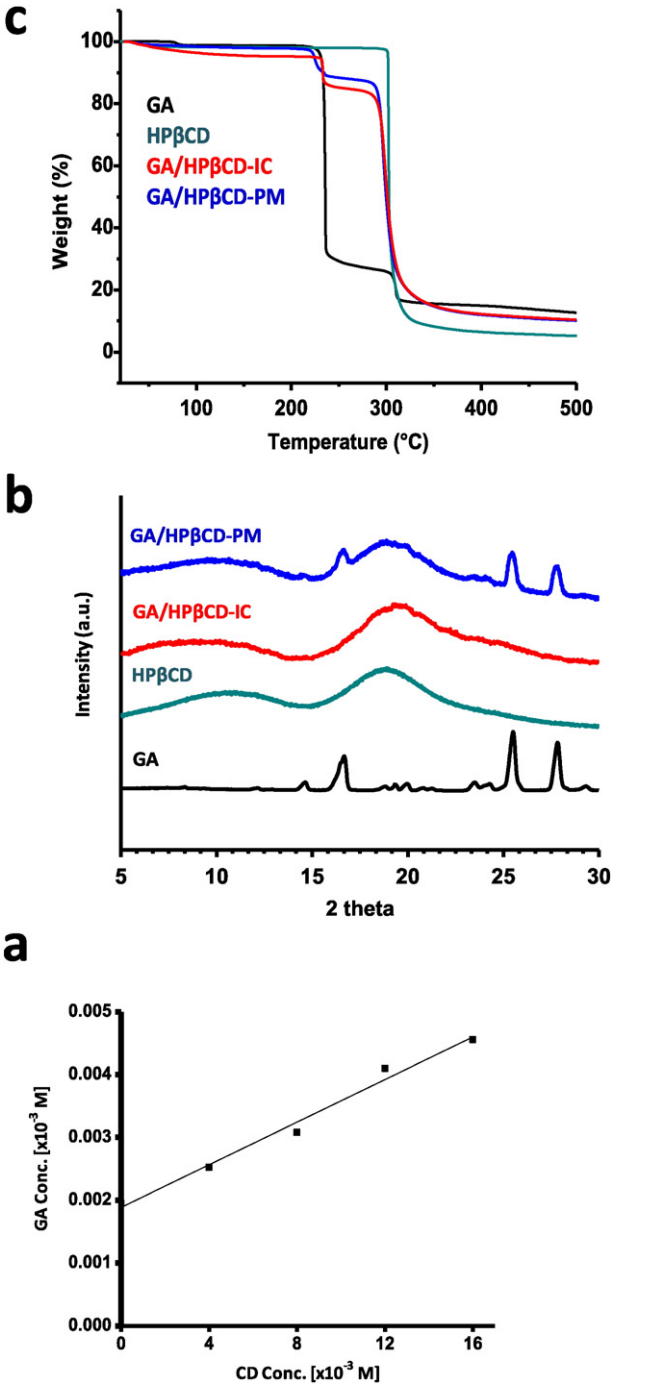

Fig. 2. (a) Phase solubility diagram of GA/HPβCD system in water, (b) XRD patterns of GA, HPβCD, GA/HPβCD-IC and GA/HPβCD-PM, (c) TGA thermograms of GA, HPβCD, GA/HPβCD-IC and GA/HPβCD-PM.

TGA thermogram, respectively. The calculated amount of GA in GA/HPβCD-IC correlates well with the initial amount of GA used for the preparation of complexation. Therefore, the initial amount of GA was preserved during the formation and storage in GA/HPβCD-IC.

3.4. The molar ratio of GA/HPβCD-IC

^{1}H NMR was used in order to determine the molar ratio of GA to HPβCD. We have shown ^{1}H NMR spectra of GA, HPβCD and GA/HPβCD-IC in Fig. 3. Firstly, ^{1}H NMR analysis was carried out for GA

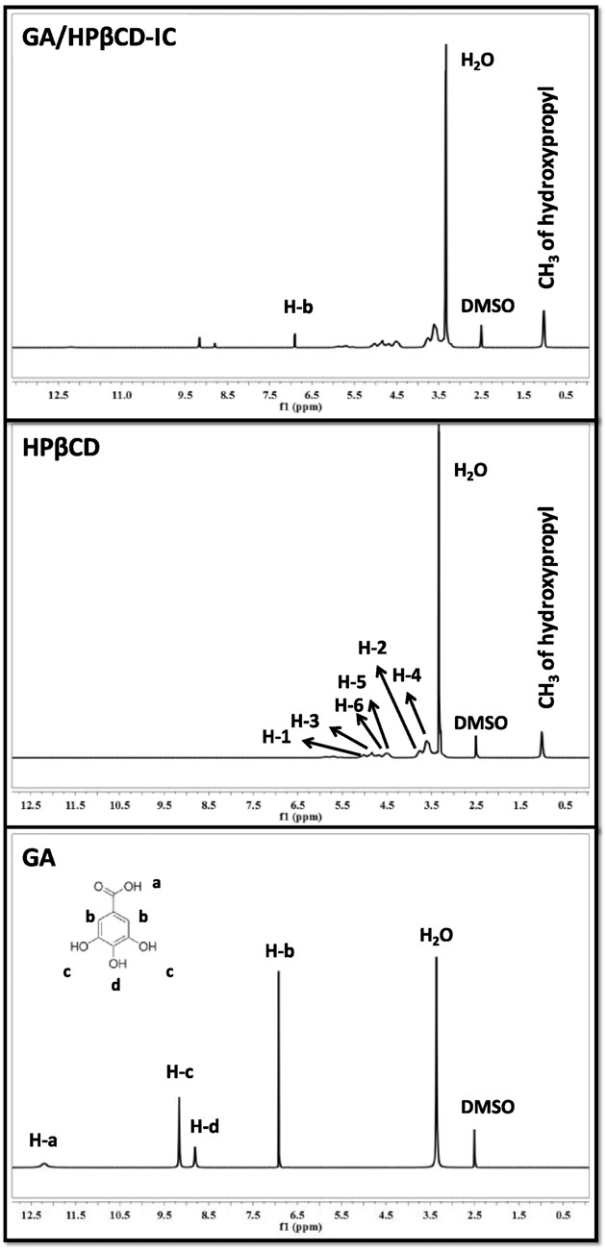

Fig. 3. ^{1}H NMR spectra of GA, HPβCD and GA/HPβCD-IC.

and HPβCD to determine the characteristic peaks of their protons. The molar ratio of GA/HPβCD-IC was decided as 0.64:1.00 (GA:HPβCD) by taking into consideration the peak ratio of the characteristic chemical shifts of GA (6.9 ppm) and HPβCD (1.0 ppm). Shortly, we revealed from the ^{1}H NMR study that the initial molar ratio of GA:HPβCD (1:1) was preserved to a great extent by complexation.

3.5. Molecular modeling of GA/HPβCD-IC

Since the inclusion of the guest molecule within HPβCD is driven by the energetics of inclusion process, we first fully optimized the initial structures of HPβCD and GA separately in vacuum. HPβCD is constructed manually by adding four 2-hydroxypropyl groups on the primary groups of β-CD corresponding to a substitution degree per anhydroglucose unit of 0.6 which was compatible with the experiments. To form IC, the guest molecule (single GA) is introduced into the cavity of HPβCD with tail and head orientations as shown in Fig. 4. The complexation energy ($E_{comp} = E_{CD} + E_{guest} - E_{IC}$), which is the difference between the total energies of HPβCD ($E_{HP\beta CD}$), the guest molecule (E_{guest}), and the inclusion complex (E_{IC}) has been calculated at various possible locations. Notably, GA prefers to stay at the center of the HPβCD cavity due to better size match. Our calculations suggest that with tail orientation stronger complexation can be formed. When compared, E_{comp} is 24.67 kcal/mol in tail orientation, thus ~15,34 kcal/mol higher than head orientation (9.33 kcal/mol). This result can be expected due to increasing polar interactions between hydroxyl groups with tail orientation. In either case, the complexation is driven by non-covalent interactions with no chemical bond formation between the guest molecule and the host (CD).

Having determined the lowest energy conformation of IC in vacuum, we also envisaged solvent effect on complexation formation of these structures. Accordingly, water is implicitly taken into consideration as solvent. All of the structures are reoptimized in water and E_{comp} is calculated. Our analysis suggested that IC can also be formed in water for both orientations. Lower E_{comp} in water when compared to vacuum can be explained by the hydrophobic nature of HPβCD cavity. A considerable electrostatic interaction occurs between solvent and GA nearby HPβCD cavity. This results in weakening of van der Waals interaction between HPβCD and GA which in turn decreases E_{comp}. Similar to vacuum case, tail orientation (15.22 kcal/mol) is energetically 12.69 kcal/mol more favorable than head orientation (2.53 kcal/mol) in solvent. In addition, the contribution of van der Waals interaction energy of GA within CD cavity in water is slightly higher (1.85 kcal/mol) for tail orientation than head orientation, suggesting more pronounced role for electrostatic interaction imposed by solvent effect of water in forming IC.

3.6. Morphology analyses of nanofibers

SEM images and AFD distributions of PLA-NF, PLA/GA-NF and PLA/GA/HPβCD-IC-NF are shown in Fig. 5. AFD of PLA-NF, PLA/GA-NF and PLA/GA/HPβCD-IC-NF were calculated to be 320 ± 115 nm, 495 ± 105 nm and 235 ± 65, respectively. The difference in the AFD of nanofibers might be related with the viscosity and conductivity of the solutions. The solution properties of PLA, PLA/GA and PLA/GA/HPβCD-IC, and the resulting electrospun nanofibers are shown in Table 1. The observed higher diameter of PLA/GA-NF as compared to PLA-NF is correlated with difference in the viscosity of solution. At the same time, it should be noted that higher conductivity might suppress the increment in the diameter of PLA/GA-NF. It is obvious that the diameter of the fiber increases upon increasing the viscosity of a solution due to the higher chain entanglement in the polymer solution [46]. On the other hand, as the conductivity of a solution increases the diameter of the nanofibers decreases owing to the increment in the number of charges leading greater stretching of the polymer jet [46]. The viscosity of PLA/GA/HPβCD-IC solution was slightly higher than PLA/GA solution; so, the diameter of PLA/GA/HPβCD-IC-NF was expected to be slightly higher than PLA/GA-NF. But considerably higher conductivity of PLA/GA/HPβCD-IC solution as compared to PLA/GA solution leads to lower diameter of PLA/GA/HPβCD-IC-NF. Moreover, encapsulation of both free GA and GA/HPβCD-IC into PLA solution did not change the morphology of nanofibers other than the increment in the AFD of nanofibers.

3.7. In vitro release study

The release of GA from PLA/GA-NF and PLA/GA/HPβCD-IC-NF into three different mediums (aqueous solution, 10% ethanol and 95% ethanol which are aqueous, alcoholic and fatty food simulants, respectively) was measured at RT via HPLC and the results are shown concentration (ppm) versus of time in Fig. 6. Loading efficiency (LE) (%) of nanofibers was determined as 80 ± 0.7% and 75 ± 0.7% for PLA/GA-NF and PLA/GA/

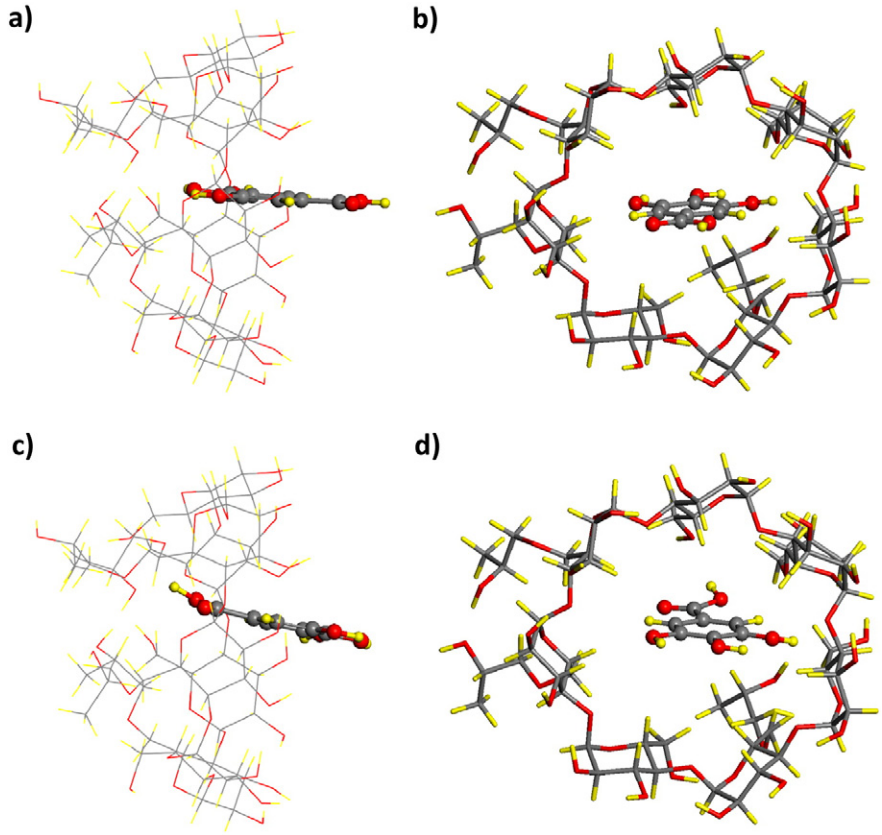

Fig. 4. Top and side view of GA/HPβCD-IC for (a)–(b) head and (c)–(d) tail orientation of GA. Gray, red, and yellow spheres represent carbon, oxygen, and hydrogen atoms, respectively.

HPβCD-IC-NF, respectively by using Eq. (2). The release of GA from PLA/GA-NF and PLA/GA/HPβCD-IC-NF shows similar behavior in all three mediums. The release of GA has reached steady state followed by fast release at the initial stage. In general, the surface area and the type of the medium are of great significance for the total amount of compound released and its release rate. In aqueous solution and 10% ethanol, higher amount of GA was released in total from PLA/GA/HPβCD-IC-NF compared to PLA/GA-NF, since CDs increase the solubility of guests as shown in Fig. 2a and the concentration of diffusible species from polymeric systems in aqueous solutions [47]. In addition, the surface area of PLA/GA/HPβCD-IC-NF was most likely higher than PLA/GA-NF due to the lower fiber diameter of PLA/GA/HPβCD-IC-NF. Therefore, the other reason of higher amount of GA released from PLA/GA/HPβCD-IC-NF could be the higher surface area of PLA/GA/HPβCD-IC-NF compared to PLA/GA-NF that provides more contact with the medium. On the other hand, the solubility of GA in ethanol is quite high [48]; therefore, PLA/GA-NF released more amount of GA in total into 95% ethanol when compared with PLA/GA/HPβCD-IC-NF. Moreover, GA released from PLA/GA-NF is the highest into 95% ethanol among the three systems.

The rate of GA released into aqueous solution and 10% ethanol was slower from PLA/GA-NF compared to PLA/GA/HPβCD-IC-NF; whereas GA released slower into 95% ethanol from PLA/GA/HPβCD-IC-NF compared with PLA/GA-NF. The difference in the rate of GA released from nanofibers was most likely due to the solubility variance of GA in different mediums. Additionally, accelerated release rate of drug was also related with the dissolution of CD-IC upon contact with water that increases the porosity of the matrix [47]. In addition, CDs not only enhance the aqueous solubility of hydrophobic guests but also act as a hydrating agent that promotes the diffusion of water into the matrix [47]. As a result, PLA/GA/HPβCD-IC-NF could be used to provide quick release into aqueous solution and 10% ethanol. At the same time this material might prevent initial oxidation and reduce the required amount of antioxidant agent due to the considerably high solubility of GA. On the contrary, PLA/GA/HPβCD-IC-NF could serve as a slow release material for 95% ethanol system.

3.8. Antioxidant activity

Phenolic compounds possess electron and/or hydrogen donor ability; therefore, they exhibit antioxidant activity. Molecules having hydroxyl groups in ortho position like GA, catechin with three hydroxyl groups bound to the aromatic ring is known to be effective phenolic compounds [49]. Here, we investigated the antioxidant capacity of GA in PLA/GA-NF and PLA/GA/HPβCD-IC-NF using DPPH radical scavenging assay. The assay is based on the reduction and neutralization of DPPH which is a stable free radical in the presence of hydrogen donating antioxidants. Furthermore, the color of DPPH solution turns into yellow with the addition of antioxidant molecule into the solution [50]. The antioxidant activity of PLA-NF, PLA/GA-NF and PLA/GA/HPβCD-IC-NF was calculated according to Eq. (3) as 4 ± 0.014%, 95 ± 0.006% and 96 ± 0.002%, respectively. The photographs of the DPPH solution before the reaction; and PLA-NF, PLA/GA-NF and PLA/GA/HPβCD-IC-NF after the reaction are shown in Fig. 7. As expected, PLA-NF had a quite low amount of antioxidant activity which might be related with the absorption of DPPH solution due to the high surface area of the nanofibers providing more contact with medium [51]. The color of the solution was still violet as shown in Fig. 7. The antioxidant activity of PLA/GA/HPβCD-IC-NF was slightly higher than PLA/GA-NF and the color of both of the solutions was pale yellow which means that there was no

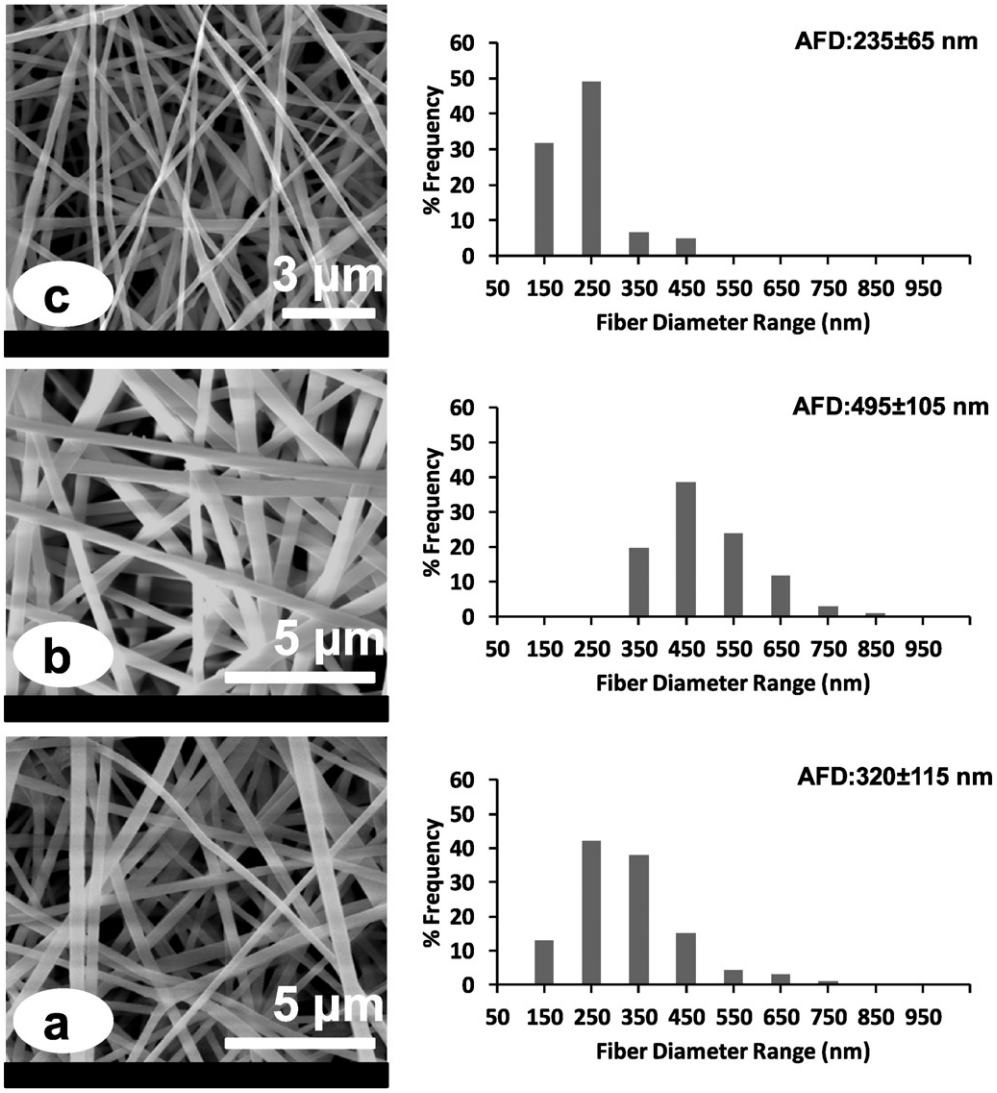

Fig. 5. SEM images and fiber diameter distributions with average fiber diameter (AFD) of electrospun nanofibers obtained from solutions of (a) PLA, (b) PLA/GA, and (c) PLA/GA/HPβCD-IC.

more DPPH molecule to deactivate in solutions. The almost same antioxidant activity of nanofibers might be explained by the quite high solubility of GA in alcohols [48] and position of GA in the cavity of CDs. According to modeling study insertion of GA into cavity from the tail orientation is energetically more favorable, so hydroxyl groups might not be in the cavity of CD. Otherwise, it is not possible for antioxidants to donate hydrogen from their hydroxyl groups to DPPH molecule and the reaction would not take place. Moreover, electrospinning had no negative effect on the antioxidant property of GA since PLA/GA-NF and PLA/GA/HPβCD-IC-NF still had a quite high amount of antioxidant activity.

4. Conclusion

Here, functional electrospun PLA nanofibers incorporating naturally occurring antioxidant compound; GA, was produced by electrospinning. The release of PLA/GA-NF and PLA/GA/HPβCD-IC-NF was evaluated in three different mediums: aqueous solution, 10% ethanol, and 95% ethanol. PLA/GA/HPβCD-IC-NF exhibited fast release of GA in aqueous solution and 10% ethanol; however, PLA/GA/HPβCD-IC-NF had shown slow release of GA in 95% ethanol. In addition, higher amount of GA release was achieved from PLA/GA/HPβCD-IC-NF in aqueous solution and 10% ethanol compared to PLA/GA-NF due to the higher solubility of GA in aqueous based systems by complexation with HPβCD. Finally, high antioxidant activity was seen for both PLA/GA/HPβCD-IC-NF and PLA/GA-NF. In brief, PLA/GA/HPβCD-IC-NF having controlled release in three different mediums and quite high antioxidant activity was successfully produced. The observed results strongly suggested that PLA/GA/HPβCD-IC-NF having an antioxidant property might be applicable as a food packaging material to increase the shelf life of food products and improve the overall food quality.

Acknowledgment

Dr. Uyar acknowledges the Scientific and Technological Research Council of Turkey (TUBITAK)-Turkey (Project no. 111M459) for funding this research. Dr. Uyar also acknowledges EU FP7-PEOPLE-2009-RG Marie Curie-IRG (NANOWEB, PIRG06-GA-2009-256428) for additional funding of the research. Dr. Uyar and Dr. Durgun acknowledge the support from The Turkish Academy of Sciences-Outstanding Young Scientists Award Program (TUBA-GEBIP)-Turkey. The calculations were performed at TUBITAK ULAKBIM, High Performance and Grid Computing Center (TR-Grid e-Infrastructure).

Z. Aytac would like to thank TUBITAK-BIDEB and TUBITAK (project nos. 111M459 and 213M185) for the PhD scholarship.

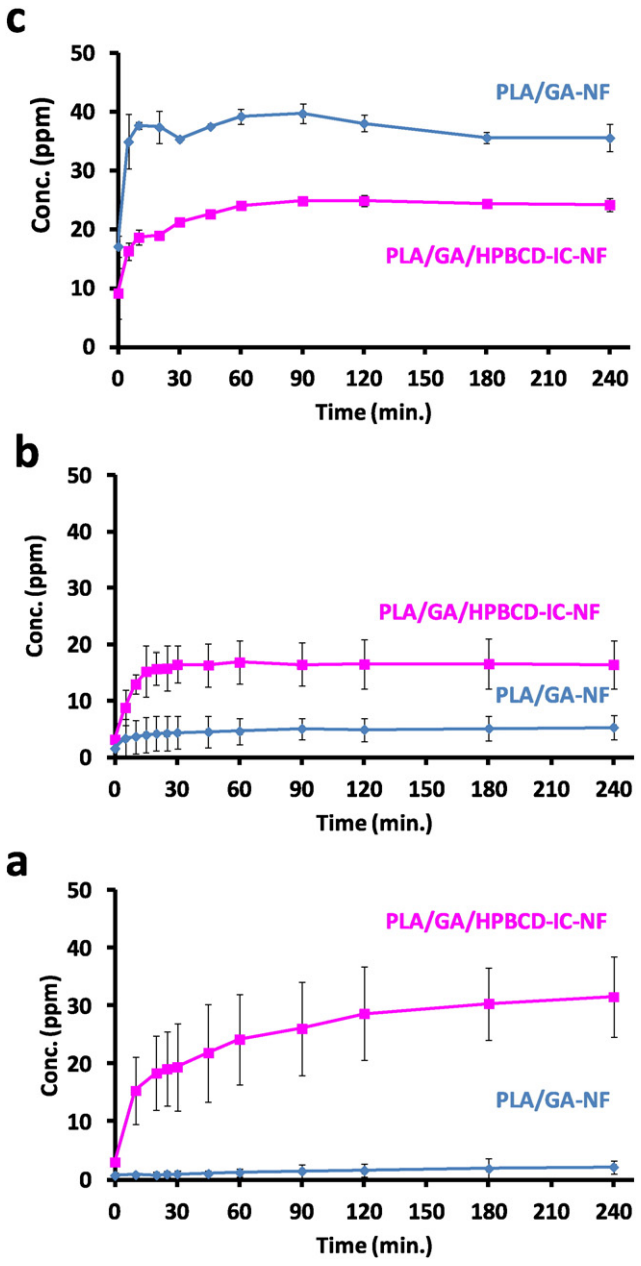

Fig. 6. The cumulative release of GA from PLA/GA-NF and PLA/GA/HPβCD-IC-NF into (a) water, (b) 10% ethanol, and (c) 95% ethanol (n = 3). The error bars in the figure represent the standard deviation (SD).

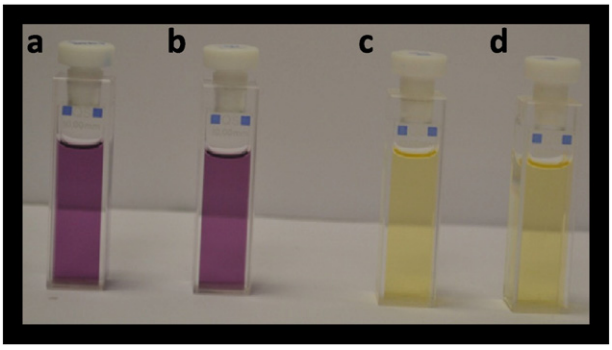

Fig. 7. The photographs of (a) DPPH solution (before the reaction); DPPH solutions in which (b) PLA-NF, (c) PLA/GA-NF and (d) PLA/GA/HPβCD-IC-NF were immersed (after the reaction).

References

[1] M. Leopoldini, N. Russo, M. Toscano, The molecular basis of working mechanism of natural polyphenolic antioxidants, Food Chem. 125 (2011) 288–306.
[2] L.A. De la Rosa, E. Alvarez-Parrilla, G.A. González-Aguilar, Fruit and vegetable phytochemicals: chemistry, nutritional value, and stability, WileyBlackwell, EUA, 2010 53–88.
[3] T. Phachamud, M. Phiriyawirut, In vitro cytotoxicity and degradability tests of gallic acid-loaded cellulose acetate electrospun fiber, Res. J. Pharm. Biol. Chem. Sci. 2 (3) (2011) 85–98.
[4] D. Alkan, L.Y. Aydemir, I. Arcan, H. Yavuzdurmaz, H.I. Atabay, C. Ceylan, A. Yemenicioğlu, Development of flexible antimicrobial packaging materials against campylobacter jejuni by incorporation of gallic acid into zein-based films, J. Agric. Food Chem. 59 (2011) 11003–11010.
[5] Y.P. Neo, S. Ray, J. Jin, M. Gizdavic-Nikolaidis, M.K. Nieuwoudt, D. Liu, S.Y. Quek, Encapsulation of food grade antioxidant in natural biopolymer by electrospinning technique: a physicochemical study based on zein-gallic acid system, Food Chem. 136 (2013) 1013–1021.
[6] Y.P. Neo, S. Swift, S. Ray, M. Gizdavic-Nikolaidis, J. Jin, C.O. Perera, Evaluation of gallic acid loaded zein sub-micron electrospun fibre mats as novel active packaging materials, Food Chem. 141 (2013) 3192–3200.
[7] E.M.M. Del Valle, Cyclodextrins and their uses: a review, Process Biochem. 39 (9) (2004) 1033–1046.
[8] C.G. Da Rosa, C.D. Borges, R.C. Zambiazi, M.R. Nunes, E.V. Benvenutti, S.R. Da Luz, R.F. D'Avila, J.K. Rutz, Microencapsulation of gallic acid in chitosan, β-cyclodextrin and xanthan, Ind. Crop. Prod. 46 (2013) 138–146.
[9] E. Pinho, G. Soares, M. Henriques, Cyclodextrin modulation of gallic acid in vitro antibacterial activity, J. Incl. Phenom. Macrocycl. Chem. 81 (2015) 205–214.
[10] M. Adabi, R. Saber, R. Faridi-Majidi, F. Faridbod, Performance of electrodes synthesized with polyacrylonitrile-based carbon nanofibers for application in electrochemical sensors and biosensors, Mater. Sci. Eng. C 48 (2015) 673–678.
[11] M. Naghibzadeh, M. Adabi, Evaluation of effective electrospinning parameters controlling gelatin nanofibers diameter via modelling artificial neural networks, Fibers Polym. 15 (4) (2014) 767–777.
[12] S.S. Esnaashari, S. Rezaei, E. Mirzaei, H. Afshari, S.M. Rezayat, R. Faridi-Majidi, Preparation and characterization of kefiran electrospun nanofibers, Int. J. Biol. Macromol. 70 (2014) 50–56.
[13] M. Adabi, R. Saber, M. Naghibzadeh, F. Faridbod, R. Faridi-Majidi, Parameters affecting carbon nanofiber electrodes for measurement of cathodic current in electrochemical sensors: an investigation using artificial neural network, RSC Adv. 5 (2015) 81243–81252.
[14] M.A. Karimi, P. Pourhakkak, M. Adabi, S. Firoozi, M. Adabi, M. Naghibzadeh, Using an artificial neural network for the evaluation of the parameters controlling PVA/chitosan electrospun nanofibers diameter, e-Polymers 15 (2) (2015) 127–138.
[15] P. Chuysinuan, N. Chimnoi, S. Techasakul, P. Supaphol, Gallic acid-loaded electrospun poly (L-lactic acid) fiber mats and their release characteristic, Macromol. Chem. Phys. 210 (2009) 814–822.
[16] I. Arcan, A. Yemenicioglu, Incorporating phenolic compounds opens a new perspective to use zein films as flexible bioactive packaging materials, Food Res. Int. 44 (2011) 550–556.
[17] J.L. Koontz, R.D. Moffitt, J.E. Marcy, S.F. O'Keefe, S.E. Duncan, T.E. Long, Controlled release of a-tocopherol, quercetin, and their cyclodextrin inclusion complexes from linear low-density polyethylene (LLDPE) films into a coconut oil model food system, Food Addit. Contam. Part A: Chem. Anal. Control Expo. Risk Assess. 27 (11) (2010) 1598–1607.
[18] Z. Aytac, H.S. Sen, E. Durgun, T. Uyar, Sulfisoxazole/cyclodextrin inclusion complex incorporated in electrospun hydroxypropyl cellulose nanofibers as drug delivery system, Colloids Surf. B: Biointerfaces 128 (2015) 331–338.
[19] R. Auras, B. Harte, S. Selke, An overview of polylactides as packaging materials, Macromol. Biosci. 4 (2004) 835–864.
[20] T. Uyar, Y. Nur, J. Hacaloglu, F. Besenbacher, Electrospinning of functional 510 poly(methyl methacrylate) nanofibers containing cyclodextrin-menthol inclusion complexes, Nanotechnology 20 (12) (2009), 125703.
[21] T. Uyar, J. Hacaloglu, F. Besenbacher, Electrospun polystyrene fibers containing high temperature stable volatile fragrance/flavor facilitated by cyclodextrin inclusion complexes, React. Funct. Polym. 69 (3) (2009) 145–150.
[22] T. Uyar, J. Hacaloglu, F. Besenbacher, Electrospun polyethylene oxide (PEO) nanofibers containing cyclodextrin inclusion complex, J. Nanosci. Nanotechnol. 11 (5) (2011) 3949–3958.
[23] F. Kayaci, T. Uyar, Encapsulation of vanillin/cyclodextrin inclusion complex in electrospun polyvinyl alcohol (PVA) nanowebs: prolonged shelf-life and high temperature stability of vanillin, Food Chem. 133 (3) (2012) 641–649.
[24] F. Kayaci, Y. Ertas, T. Uyar, Enhanced thermal stability of eugenol by cyclodextrin inclusion complex encapsulated in electrospun polymeric nanofibers, J. Agric. Food Chem. 61 (34) (2013) 8156–8165.
[25] F. Kayaci, O.C.O. Umu, T. Tekinay, T. Uyar, Antibacterial electrospun poly(lactic acid) (PLA) nanofibrous webs Incorporating triclosan/cyclodextrin inclusion complexes, J. Agric. Food Chem. 61 (16) (2013) 3901–3908.
[26] F. Kayaci, H.S. Sen, E. Durgun, T. Uyar, Functional electrospun polymeric nanofibers incorporating geraniol-cyclodextrin inclusion complexes: high thermal stability and enhanced durability of geraniol, Food Res. Int. 62 (2014) 424–431.
[27] M.F. Canbolat, A. Celebioglu, T. Uyar, Drug delivery system based on cyclodextrin-naproxen inclusion complex incorporated in electrospun polycaprolactone nanofibers, Colloids Surf. B: Biointerfaces 115 (2014) 15–21.
[28] Z. Aytac, S.Y. Dogan, T. Tekinay, T. Uyar, Release and antibacterial activity of allyl isothiocyanate/β-cyclodextrin inclusion complex encapsulated in electrospun nanofibers, Colloids Surf. B: Biointerfaces 120 (2014) 125–131.

[29] T. Higuchi, A.K. Connors, Phase-solubility techniques, Adv. Anal. Chem. Instrum. 4 (1965) 117–212.
[30] W. Kohn, L.J. Sham, Self-consistent equations including exchange and correlation effects, Phys. Rev. 140 (1965) A1133–A1138.
[31] P. Hohenberg, W. Kohn, Inhomogeneous electron gas, Phys. Rev. 136 (1964) B864–B871.
[32] J.P. Perdew, J.A. Chevary, S.H. Vosko, K.A. Jackson, M.R. Pederson, D.J. Singh, C. Fiolhais, Atoms, molecules, solids, and surfaces: applications of the generalized gradient approximation for exchange and correlation, Phys. Rev. B 46 (1992) 6671–6687.
[33] S. Grimme, Semiempirical GGA-type density functional constructed with a long-range dispersion correction, J. Comput. Chem. 27 (15) (2006) 1787–1799.
[34] G. Kresse, J. Furthmüller, Efficient iterative schemes for ab initio total-energy calculations using a plane-wave basis set, Phys. Rev. B 54 (16) (1996) 11169–11186.
[35] G. Kresse, J. Furthmüller, Efficiency of ab-initio total energy calculations for metals and semiconductors using a plane-wave basis set, Comput. Mater. Sci. 6 (1) (1996) 15–50.
[36] P.E. Blöchl, Projector augmented-wave method, Phys. Rev. B 50 (24) (1994) 17953–17979.
[37] F.H. Allen, The Cambridge structural database: a quarter of a million crystal structures and rising, Acta Crystallogr. Sect. B: Struct. Sci. 58 (3) (2002) 380–388.
[38] J.L. Fattebert, F. Gygi, First-principles molecular dynamics simulations in a continuum solvent, Int. J. Quantum Chem. 93 (2) (2003) 139–147.
[39] O. Andreussi, I. Dabo, N. Marzari, Revised self-consistent continuum solvation in electronic-structure calculations, J. Chem. Phys. 136 (2012) 064102.
[40] S.A. Petrosyan, A.A. Rigos, T.A. Arias, Joint density-functional theory: ab initio study of Cr_2O_3 surface chemistry in solution, J. Phys. Chem. B 109 (32) (2005) 15436–15444.
[41] K. Mathew, R. Sundararaman, K. Letchworth-Weaver, T.A. Arias, R.G. Hennig, Implicit solvation model for density-functional study of nanocrystal surfaces and reaction pathways, J. Chem. Phys. 140 (2014) 084106.
[42] V.J. Stella, V.M. Rao, E.A. Zannou, V. Zia, Mechanisms of drug release from cyclodextrin complexes, Adv. Drug Deliv. Rev. 36 (1) (1999) 3–16.
[43] F. Giordano, C. Novak, J.R. Moyano, Thermal analysis of cyclodextrins and their inclusion compounds, Thermochim. Acta 380 (2) (2001) 123–151.
[44] E.E. Eid, A.B. Abdul, F.E.O. Suliman, M.A. Sukari, A. Rasedee, S.S. Fatah, Characterization of the inclusion complex of zerumbone with hydroxypropyl-β-cyclodextrin, Carbohydr. Polym. 83 (4) (2011) 1707–1714.
[45] J.-Y. Tsao, C.-P. Wu, H.-H. Tsai, K.-C. Peng, P.-Y. Lin, S.-Y. Su, L.-D. Chen, F.-J. Tsai, Y. Tsai, Effect of hydroxypropyl-β-cyclodextrin complexation on the aqueous solubility, structure, thermal stability, antioxidant activity, and tyrosinase inhibition of paeonol, J. Incl. Phenom. Macrocycl. Chem. 72 (3) (2012) 405–411.
[46] S. Ramakrishna, K. Fujihara, W.-E. Teo, T.-C. Lim, Z. Ma, An Introduction to Electrospinning and Nanofibers, 90World Scientific, Singapore, 2005.
[47] D.C. Bibby, N.M. Davies, I.G. Tucker, Mechanisms by which cyclodextrins modify drug release from polymeric drug delivery systems, Int. J. Pharm. 197 (1-2) (2000) 1–11.
[48] A. Daneshfar, H.S. Ghaziaskar, N. Homayoun, Solubility of gallic acid in methanol, ethanol, water, and ethyl acetate, J. Chem. Eng. Data 53 (3) (2008) 776–778.
[49] R.E. Ghitescu, A.M. Popa, V.I. Popa, R.M. Rossi, G. Fortunato, Encapsulation of polyphenols into pHEMA e-spun fibers and determination of their antioxidant activities, Int. J. Pharm. 494 (2015) 278–287.
[50] K. Mishra, H. Ojha, N.K. Chaudhury, Estimation of antiradical properties of antioxidants using DPPH assay: a critical review and results, Food Chem. 130 (2012) 1036–1043.
[51] S. Banerjee, J.P. Saikia, A. Kumar, B. Konwar, Antioxidant activity and haemolysis prevention efficiency of polyaniline nanofibers, Nanotechnology 21 (4) (2010) 045101.